SIAM J. APPL. MATH.
Vol. 63, No. 1, pp. 98–115

DESORPTION OVERSHOOT IN POLYMER-PENETRANT SYSTEMS: ASYMPTOTIC AND COMPUTATIONAL RESULTS*

DAVID A. EDWARDS† AND RICHARD A. CAIRNCROSS‡

Abstract. Many practically relevant polymers undergoing desorption change from the rubbery (saturated) to the glassy (nearly dry) state. The dynamics of such systems cannot be described by the simple Fickian diffusion equation due to viscoelastic effects. The mathematical model solved numerically is a set of two coupled PDEs for concentration and stress. Asymptotic solutions are presented for a moving boundary-value problem for the two states in the short-time limit. The solutions exhibit *desorption overshoot*, where the penetrant concentration in the interior is less than that on the surface. In addition, it is shown that if the underlying time scale of the equations is ignored when postulating boundary conditions, nonphysical solutions can result.

Key words. asymptotic expansions, desorption, moving boundary-value problems, perturbation methods, polymer-penetrant systems, finite-element method

AMS subject classifications. 35B20, 35C15, 35C20, 35K60, 35R35, 65N30, 74D10, 76M10, 76R99, 80A22

PII. S0036139901390428

1. Introduction.

Over the past few decades, much experimental and theoretical work has been devoted to the study of polymer-penetrant systems. In particular, the desorption of penetrants from saturated polymer matrices has been examined due to its wide industrial applicability. One unusual feature of such systems is the change in the polymer from a *rubbery* state when it is nearly saturated to a *glassy* state when it is nearly dry. As part of the drying process, a glassy *skin* often develops at the exposed surface of a polymer whose properties are significantly different from the rest of the polymer-penetrant solution [1], [2], [3], [4], [5]. This phenomenon, called *skinning* [6], [7], [8], has many industrial applications [8], [9], [10], [11], [12], [13], [14], [15], [16].

There are many different theories for why the skinning process occurs, including phase separation [17], crystallization [18], and diffusion-induced convection [19]. Nevertheless, for the systems we wish to study, most scientists agree that one important factor is a viscoelastic stress in the polymer entanglement network, which can be as important to the transport process as the well-understood Fickian dynamics [20], [21], [22]. The size of this stress is related to the *relaxation time* of the viscoelastic polymer matrix. In the glassy skin, the relaxation time is finite, so the stress is an important effect, but in the rubbery region the relaxation time is nearly zero [15], [20], [23]. Nevertheless, we will show that in order for the mathematical model to yield physically meaningful results, at some level the short relaxation time in the rubber must also be taken into account.

Numerical and analytical solutions are derived here for model equations for the

*Received by the editors June 6, 2001; accepted for publication (in revised form) January 21, 2002; published electronically August 5, 2002.

http://www.siam.org/journals/siap/63-1/39042.html

†Department of Mathematical Sciences, University of Delaware, Newark, DE 19716-2553 (edwards@math.udel.edu). The work of this author was supported by the National Science Foundation grant DMS-9972013.

‡Department of Chemical Engineering, Drexel University, 3141 Chestnut Street, Philadelphia, PA 19104 (cairncro@coe.drexel.edu). The work of this author was supported by a 3M Non-Tenured Faculty Grant.

system described above. Our equations are the same, to leading order, as those for general polymer-penetrant systems derived in detail by Edwards and Cohen [24], [25], Edwards [26], Cairncross and Durning [8], Durning [27], and Durning and Tabor [28]. These models, which are presented in section 2, consist of a set of coupled PDEs for the concentration and stress. The parameters in the numerical simulation vary smoothly with concentration, so the glass-rubber interface $x = s(t)$ between the two states is simply an isocline of concentration. In contrast, the parameters in the analytical model are assumed to be piecewise constant in the rubber and glass. Thus, a moving boundary-value problem similar to a Stefan problem results. In each of the regions a different partial differential operator holds, and continuity conditions at the glass-rubber interface dictate its motion.

In section 3 we construct a perturbation solution to the equations. The solutions are expressed as integrals of Green's functions convolved with fictitious boundary conditions which provide the new unknowns for which we must solve. In section 4 we construct short-time asymptotic solutions of the concentration and stress fields. The form of the short-time solutions necessitates a corner layer, where the full system of equations holds. The solutions exhibit *desorption overshoot*, where the minimum in the concentration occurs in the interior of the domain.

In addition, if we use a standard high-mass-transfer-coefficient approximation common in diffusion and heat conduction problems, it is possible for the concentration to become negative. This result is confirmed numerically in section 5. In section 6 it is explained that the unphysical negative concentration appears because the limit of high mass transfer coefficient imposes a jump in the exterior concentration faster than the underlying time scales of the operator. Physically, the polymer is *self-regulating* for desorption as well as sorption [24]. A new boundary condition is postulated which incorporates the time scale in the stress evolution equation, and it is shown that such a boundary condition does not lead to negative concentrations.

2. Preliminaries.

2.1. Governing equations.

We examine the following dimensionless system of equations for anomalous desorption in a polymer of finite dimensionless length L:

$$\frac{\partial C}{\partial t} = \frac{\partial}{\partial x}\left(D(C)\frac{\partial C}{\partial x} + \frac{\partial \sigma}{\partial x}\right), \qquad 0 \le x \le L, \tag{2.1a}$$

$$\frac{\partial \sigma}{\partial t} + \frac{\beta(C)}{\beta_{\mathrm{g}}}\sigma = \gamma\epsilon C + \frac{\partial C}{\partial t}, \tag{2.1b}$$

where C is the dimensionless concentration of penetrant in the polymer, γ is a dimensionless constant, and L is the length of the slab scaled with the length scale of stress evolution [29].

The system is described in general in [29] and specialized in [26], but some discussion is required. The flux in (2.1a) can be derived by postulating that the chemical potential is a function of both C and σ [24], which in one dimension corresponds to the stress in the polymer network [24], [30], [31], [32]. In (2.1b), the coefficient of $\partial\sigma/\partial x$ has been chosen constant, in contrast to the models of Durning and colleagues [8], [28], [33].

$D(C)$ is a normalized diffusion coefficient measuring the ratio of the Fickian to non-Fickian effects in the flux. Also $\beta(C)$ is the inverse of the relaxation time, which measures the speed at which changes in one part of the polymer are communicated

to other parts of the polymer. Both increase dramatically as the polymer goes from the glassy to rubbery state [15], [20], [23], [34], [35], [36]. In contrast, the differences in these parameters *within* states are qualitatively negligible. Therefore, for our numerical work we assume the following forms for these functions:

$$\begin{aligned} D(C) &= D_{\mathrm{g}} - \frac{D_{\mathrm{g}} - D_{\mathrm{r}}}{2}\left[1 + \tanh(\alpha(C - C_*))\right], \\ \beta(C) &= \beta_{\mathrm{g}} - \frac{\beta_{\mathrm{g}} - \beta_{\mathrm{r}}}{2}\left[1 + \tanh(\alpha(C - C_*))\right], \end{aligned} \qquad \alpha \gg 1, \tag{2.2}$$

where C_* is the value of the concentration at which the glass-rubber transition occurs. Other physically appropriate forms for β and D are presented in [4], [8], [28], [33], [34], [35], [36], [37].

We examine a polymer that is initially saturated (and hence rubbery) and unstressed, which leads to the initial conditions

$$C^{\mathrm{r}}(x,0) = 1, \qquad \sigma^{\mathrm{r}}(x,0) = 0. \tag{2.3}$$

The end $x = L$ is insulated, while at the exposed surface $x = 0$, the flux is proportional to the difference between the surface concentration and the environment concentration C_{ext}:

$$\left(D(C)\frac{\partial C}{\partial x} + \frac{\partial \sigma}{\partial x}\right)(L,t) = 0, \tag{2.4a}$$

$$\left(D(C)\frac{\partial C}{\partial x} + \frac{\partial \sigma}{\partial x}\right)(0,t) = k[C(0,t) - C_{\mathrm{ext}}], \tag{2.4b}$$

where k is a constant measuring the mass transfer coefficient of the exposed interface.

2.2. Two-state formulation. We solve (2.1)–(2.4) numerically in section 5, but in order to obtain direct dependence of our solution on the physical parameters in the system, we will solve the problem analytically, which necessitates some simplifications.

As $\alpha \to \infty$, the parameters in (2.2) become piecewise constant:

$$\begin{aligned} D(C) &= \begin{cases} D_0\epsilon, & 0 \le C \le C_*, \\ D_{\mathrm{r}}, & C_* \le C \le 1, \end{cases} \\ \beta(C) &= \begin{cases} \beta_{\mathrm{g}}, & 0 \le C \le C_*, \\ \beta_{\mathrm{r}}, & C_* < C \le 1. \end{cases} \end{aligned} \tag{2.5}$$

The rubber is closest to the Fickian regime because the relaxation time is almost instantaneous; thus $\beta_{\mathrm{g}}/\beta_{\mathrm{r}} = \epsilon \ll 1$. It has been shown experimentally [16] that the diffusion coefficient in the glassy region is quite small, so we let $D_{\mathrm{g}} = D_0\epsilon$, where D_0 is an $O(1)$ constant.

With the functional forms in (2.5), it is natural to model the physical system as a two-state problem with a moving boundary $x = s(t)$ representing the glass-rubber interface. Thus, making our substitutions into (2.1), we obtain the following in the glassy region:

$$\frac{\partial C^{\mathrm{g}}}{\partial t} = D_0\epsilon\frac{\partial^2 C^{\mathrm{g}}}{\partial x^2} + \frac{\partial^2 \sigma^{\mathrm{g}}}{\partial x^2}, \tag{2.6a}$$

$$\frac{\partial \sigma^{\mathrm{g}}}{\partial t} + \sigma^{\mathrm{g}} = \gamma\epsilon C^{\mathrm{g}} + \frac{\partial C^{\mathrm{g}}}{\partial t}, \tag{2.6b}$$

while in the rubbery region we have

$$\frac{\partial C^{\mathrm{r}}}{\partial t} = D_{\mathrm{r}} \frac{\partial^2 C^{\mathrm{r}}}{\partial x^2} + \frac{\partial^2 \sigma^{\mathrm{r}}}{\partial x^2}, \tag{2.7a}$$

$$\frac{\partial \sigma^{\mathrm{r}}}{\partial t} + \frac{\sigma^{\mathrm{r}}}{\epsilon} = \gamma \epsilon C^{\mathrm{r}} + \frac{\partial C^{\mathrm{r}}}{\partial t}. \tag{2.7b}$$

With such a formulation, we must have conditions that hold at $x = s(t)$. We impose continuity of concentration at the glass-rubber transition value C_*:

$$C^{\mathrm{r}}(s(t), t) = C^{\mathrm{g}}(s(t), t) = C_*. \tag{2.8}$$

In addition, we require continuity of stress and flux:

$$\sigma^{\mathrm{r}}(s(t), t) = \sigma^{\mathrm{g}}(s(t), t), \tag{2.9a}$$

$$\left(D_{\mathrm{r}} \frac{\partial C^{\mathrm{r}}}{\partial x} + \frac{\partial \sigma^{\mathrm{r}}}{\partial x} \right)(s(t), t) = \left(D_0 \epsilon \frac{\partial C^{\mathrm{g}}}{\partial x} + \frac{\partial \sigma^{\mathrm{g}}}{\partial x} \right)(s(t), t). \tag{2.9b}$$

3. Perturbation solution. We assume perturbation expansions for our dependent variables in ϵ, the small ratio of the relaxation times:

$$C \sim C_0 + O(\epsilon), \qquad \sigma \sim \sigma_0 + O(\epsilon), \tag{3.1}$$

where the same expansions hold for the rubber and glass.

3.1. The glassy region. Substituting (3.1) into (2.6) yields

$$\frac{\partial C_0^{\mathrm{g}}}{\partial t} = \frac{\partial^2 \sigma_0^{\mathrm{g}}}{\partial x^2}, \tag{3.2a}$$

$$\frac{\partial \sigma_0^{\mathrm{g}}}{\partial t} + \sigma_0^{\mathrm{g}} = \frac{\partial C_0^{\mathrm{g}}}{\partial t}. \tag{3.2b}$$

It is simpler to solve for the stress in the glassy region first; hence we combine (3.2) to obtain

$$\frac{\partial \sigma_0^{\mathrm{g}}}{\partial t} + \sigma_0^{\mathrm{g}} = \frac{\partial^2 \sigma_0^{\mathrm{g}}}{\partial x^2}, \qquad 0 < x < s(t). \tag{3.3}$$

In many industrial applications, fast drying is desirable in order to reduce production time and cost. Thus, we consider the case where $k \to \infty$, which corresponds to high mass transfer coefficient or large driving force. (In certain scaling limits, this can also correspond to thick films.) Making this substitution in (2.4b), we obtain

$$C_0^{\mathrm{g}}(0, t) = C_{\mathrm{ext}} < C_*, \tag{3.4}$$

which locates the glass-rubber interface at the origin for $t = 0$. This sort of Dirichlet condition is routinely used in diffusion or heat conduction problems, instead of the more physically realistic flux or activity balance conditions. Nevertheless, we shall see that in this context, imposing such a simple boundary condition can produce unphysical results.

Equation (3.4) implies that the concentration jumps discontinuously at the origin from 1 to C_{ext}, so we have the following:

$$\frac{dC}{dt}(0,t) = (C_{\text{ext}} - 1)\delta(t), \tag{3.5}$$

and upon substituting this result into (3.2b) evaluated at $x = 0$, we obtain

$$\sigma_0^{\text{g}}(0,t) = (C_{\text{ext}} - 1)e^{-t}. \tag{3.6}$$

Note the exponential decay of surface stress from its initial value, reflecting the memory effects in the glassy polymer.

In order to solve the problem, we use an integral method first introduced by Boley [38] and used extensively in this context by Edwards and Cohen [24] and Edwards [26], [29], [39], [40]. Essentially, we wish to write the solution of (3.3) and (3.6) as a Green's function convolved with a *fictitious* initial condition $\sigma_0^{\text{g}}(x,0) = f^{\text{i}}(x)$. This condition is fictitious because the polymer is not glassy at $t = 0$. Thus we extend our domain beyond the region $0 < x < s(t)$. By writing our solution in this form, we reduce the problem from a PDE to an integrodifferential equation.

Since all expressions for $x > s(t)$ are fictitious anyway, we embed the problem in the semi-infinite domain $x > 0$. The solution then is found to be

$$\sigma_0^{\text{g}}(x,t) = (C_{\text{ext}} - 1)e^{-t}\operatorname{erfc}\left(\frac{x}{2\sqrt{t}}\right)$$

$$+\frac{e^{-t}}{2\sqrt{\pi t}}\int_0^\infty f^{\text{i}}(z)\left\{\exp\left[-\frac{(x-z)^2}{4t}\right] - \exp\left[-\frac{(x+z)^2}{4t}\right]\right\}dz. \tag{3.7}$$

3.2. The rubbery region. In the rubbery region we substitute (3.1) into (2.7b) to obtain

$$\sigma_0^{\text{r}}(x,t) = 0. \tag{3.8}$$

Since the γ term does not contribute to the dynamics in either the glassy or the rubbery regions, our model (2.1) contains exactly those dynamical processes as in the models of Cairncross and Durning [8], Durning [27], and Durning and Tabor [28].

Substituting (3.1) and (3.8) into (2.7a) yields

$$\frac{\partial C_0^{\text{r}}}{\partial t} = D_{\text{r}}\frac{\partial^2 C_0^{\text{r}}}{\partial x^2}, \qquad s(t) < x < L, \quad 0 < t < t_L, \tag{3.9a}$$

where $s(t_L) = L$. To use Boley's method to rewrite our solution, we note that upon substituting (3.1) and (3.8) into (2.4a), we obtain

$$\frac{\partial C_0^{\text{r}}}{\partial x}(L,t) = 0, \tag{3.9b}$$

and hence $x = L$ is a line of symmetry. Thus by the method of images

$$C_0^{\text{r}}(x,t) = 1 - [T^{\text{r}}(x,t) + T^{\text{r}}(2L - x,t)] \tag{3.10a}$$

is a solution to (3.9) and (2.3) if $T^{\text{r}}(x,t)$ is a solution of the heat equation. Since the rubber occupies the region $s(t) < x < L$, the fictitious condition is $T^{\text{r}}(0,t) = f^{\text{b}}(t)$, so T^{r} is given by

$$T^{\text{r}}(x,t) = \frac{x}{2\sqrt{D_{\text{r}}\pi}}\int_0^t \frac{f^{\text{b}}(z)}{(t-z)^{3/2}}\exp\left[-\frac{x^2}{4D_{\text{r}}(t-z)}\right]dz. \tag{3.10b}$$

Substituting (3.1) and (3.8) into (2.8) and (2.9), we obtain

$$C_0^{\mathrm{r}}(s(t),t) = C_0^{\mathrm{g}}(s(t),t) = C_*, \tag{3.11a}$$

$$\sigma_0^{\mathrm{g}}(s(t),t) = 0, \tag{3.11b}$$

$$D_{\mathrm{r}}\frac{\partial C_0^{\mathrm{r}}}{\partial x}(s(t),t) = \frac{\partial \sigma_0^{\mathrm{g}}}{\partial x}(s(t),t). \tag{3.12}$$

Upon substitution of (3.7) and (3.10) into (3.11) and (3.12), we will obtain three integrodifferential equations for the unknowns f^{i}, f^{b}, and s.

4. Short-time solutions.

4.1. The outer solution. We examine the small-time asymptotics of our analytic solution as in Edwards [26] by letting

$$f^{\mathrm{i}}(x) \sim f_0^{\mathrm{i}}, \qquad f^{\mathrm{b}}(t) \sim f_0^{\mathrm{b}}, \qquad s(t) = 2s_0 t^n, \qquad t \to 0, \quad x \to 0. \tag{4.1}$$

We substitute (4.1) into (3.10) and (3.7) to obtain expressions for our unknowns for $L = O(1)$. Substituting these expressions into (3.11) and (3.12), we obtain

$$C_* \sim 1 - f_0^{\mathrm{b}} \operatorname{erfc}\left(\frac{s_0 t^{n-1/2}}{\sqrt{D_{\mathrm{r}}}}\right), \tag{4.2a}$$

$$0 \sim (C_{\mathrm{ext}} - 1)\operatorname{erfc}(s_0 t^{n-1/2}) + f_0^{\mathrm{i}} \operatorname{erf}(s_0 t^{n-1/2}), \tag{4.2b}$$

$$\frac{D_{\mathrm{r}} f_0^{\mathrm{b}}}{\sqrt{\pi D_{\mathrm{r}} t}} \exp\left(-\frac{s^2}{4D_{\mathrm{r}} t}\right) \sim [f_0^{\mathrm{i}} - (C_{\mathrm{ext}} - 1)]\frac{e^{-t}}{\sqrt{\pi t}} \exp\left(-\frac{s^2}{4t}\right). \tag{4.3}$$

Equation (4.2a) can be satisfied if and only if $n \geq 1/2$. Equation (4.2b) can be satisfied if and only if $n \leq 1/2$. Therefore $n = 1/2$ and initially the front moves in a purely Fickian way because the nonlinear memory effects have not yet had time to develop. Using this result, we obtain

$$g_1(s_0) \equiv \sqrt{D_{\mathrm{r}}}\frac{1 - C_*}{\operatorname{erfc}(s_0/\sqrt{D_{\mathrm{r}}})} \exp\left(-\frac{s_0^2}{D_{\mathrm{r}}}\right) = \frac{1 - C_{\mathrm{ext}}}{\operatorname{erf} s_0} \exp\left(-s_0^2\right) \equiv g_2(s_0). \tag{4.4}$$

Figure 4.1 shows plots of $g_2 - g_1$ for various values of C_*. The s_0-intercept marks the value of the front speed. Note that as C_* increases, the front speed increases since not as much penetrant has to desorb to move the front along.

Figure 4.2 shows the variance in the front speed as D_{r} and C_{ext} vary. Note that as C_{ext} decreases, the front speed increases because of a larger driving force. In addition, as D_{r} increases, the front speed decreases because it is easier to diffuse penetrant to the front.

Using (4.4), we may derive the value of f_0^{b} and hence obtain

$$C_0^{\mathrm{r}}(x,t) = 1 - \frac{1 - C_*}{\operatorname{erfc}(s_0/\sqrt{D_{\mathrm{r}}})}\left[\operatorname{erfc}\left(\frac{x}{2\sqrt{D_{\mathrm{r}} t}}\right) + \operatorname{erfc}\left(\frac{2L - x}{2\sqrt{D_{\mathrm{r}} t}}\right)\right]. \tag{4.5}$$

As $L \to \infty$, the second term drops out and we are left with exactly the expression in Edwards [26] for the case of a semi-infinite domain. In addition, as $t \to 0$ the second term modeling "reflections" from $x = L$ is negligible.

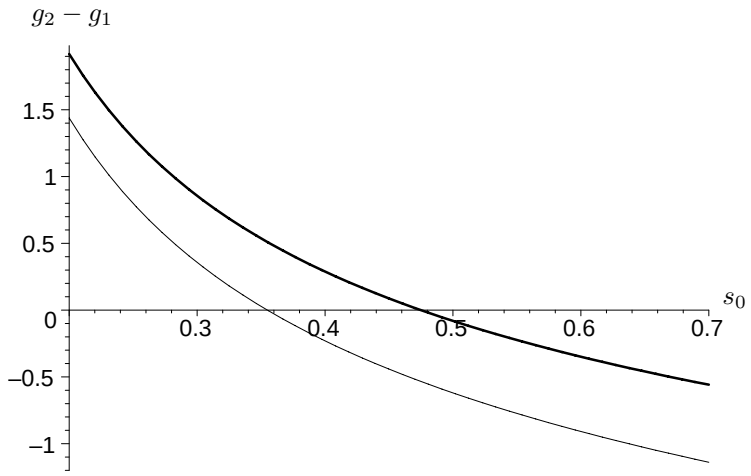

FIG. 4.1. $g_2 - g_1$ *versus* s_0 *for* $D_\mathrm{r} = 7$, $C_\mathrm{ext} = 1/3$. *Thin line:* $C_* = 1/2$. *Thick line:* $C_* = 2/3$.

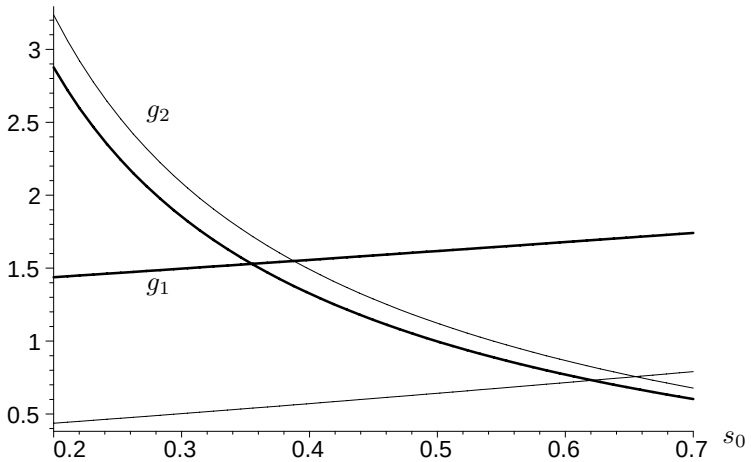

FIG. 4.2. g_1 *and* g_2 *versus* s_0 *for* $C_* = 1/2$. *Thick lines:* $D_\mathrm{r} = 0.4$, $C_\mathrm{ext} = 1/4$. *Thin lines:* $D_\mathrm{r} = 7$, $C_\mathrm{ext} = 1/3$.

We may also use (4.4) to derive the value of f_0^i and hence obtain

$$\sigma_0^\mathrm{g}(x,t) \sim (C_\mathrm{ext} - 1)e^{-t}\left[1 - \frac{1}{\operatorname{erf} s_0}\operatorname{erf}\left(\frac{x}{2\sqrt{t}}\right)\right]. \tag{4.6}$$

Substituting (4.6) into (3.2a) and solving using (3.11a), we have the following:

$$\begin{aligned} C^\mathrm{g}(x,t) = C_* + \frac{C_\mathrm{ext} - 1}{2\operatorname{erf} s_0}\Bigg\{ & e^{-x}\left[\operatorname{erfc}\left(-\sqrt{t} + \frac{x}{2\sqrt{t}}\right) - \operatorname{erfc}\left(s_0 - \frac{x}{2s_0}\right)\right] \\ & + e^{x}\left[\operatorname{erfc}\left(\sqrt{t} + \frac{x}{2\sqrt{t}}\right) - \operatorname{erfc}\left(s_0 + \frac{x}{2s_0}\right)\right]\Bigg\}, \end{aligned} \tag{4.7}$$

where the x/s_0 terms come from the asymptotic expansion of $s^{-1}(x)$, the inverse function for the front position:

$$s^{-1}(x) \sim \left(\frac{x}{2s_0}\right)^2, \qquad x \to 0. \tag{4.8}$$

Unfortunately, we note that if we substitute $x = 0$ into (4.7), we obtain

$$\lim_{x\to 0} C_0^{\mathrm{g}}(x,t) = C_* + C_{\mathrm{ext}} - 1 \neq C_{\mathrm{ext}} = C^{\mathrm{g}}(0,t). \tag{4.9}$$

The discontinuity near $x = 0$ must be resolved by a boundary layer, but even the solution to the full problem near $x = 0$ will be less than C_{ext}. We call this excessive drying near the exposed surface *desorption overshoot*, as the minimum of the concentration now occurs inside the film. The terminology is motivated by the related phenomenon of *sorption overshoot*, where the concentration rises above its equilibrium value during a sorption experiment [41].

Moreover, it is certainly possible for $C_* + C_{\mathrm{ext}} - 1 < 0$, which would yield the physically unrealistic result of a negative concentration. This unphysical aspect is not an artifact of the asymptotics; rather it is the direct result of the Dirichlet condition (3.4), as discussed in section 6.

4.2. The corner layer. The discontinuity about $x = 0$ is caused by the form of the operator in (3.2a). As long as the evolution equation for C has only a $\partial C/\partial t$ term in it, then σ and C will differ *everywhere* only by a function of x. Since both C and σ_0^{r} are constants along the front, that difference must also be a constant at the front. This causes a discontinuity because

$$\lim_{t\to 0} C(s(t),t) \neq \lim_{t\to 0} C(0,t).$$

σ_0^{r} does not vary along the front due to the ϵ^{-1} term in (2.7b). This term can be counteracted if we introduce a corner layer near the origin *via* the following substitutions:

$$C^{\mathrm{r}}(x,t) = C^+(\xi,\tau), \qquad \sigma^{\mathrm{r}}(x,t) = \sigma^+(\xi,\tau), \qquad \xi = \frac{x}{\epsilon^{1/2}}, \qquad \tau = \frac{t}{\epsilon}. \tag{4.10}$$

Substituting (4.10) into (2.7), we obtain

$$\frac{\partial C^+}{\partial \tau} = D_{\mathrm{r}} \frac{\partial^2 C^+}{\partial \xi^2} + \frac{\partial^2 \sigma^+}{\partial \xi^2}, \tag{4.11a}$$

$$\frac{\partial \sigma^+}{\partial \tau} + \sigma^+ = \frac{\partial C^+}{\partial \tau}, \tag{4.11b}$$

which is just the full system (2.7) without the γ term. Hence even in the corner layer, our model matches that of Cairncross and Durning [8], Durning [27], and Durning and Tabor [28]. Note that τ is the time scale for relaxation in the rubber.

To solve this system, we must proceed numerically. Nevertheless, we note that due to the exponential decay inherent in (4.11b), curves of constant C are not curves of constant σ. This fact will remove the discontinuity, which was caused by the fact that the front was an isocline for both outer solutions.

5. Numerical computations. We compare our asymptotic results to those from a finite-element code previously used to solve a similar model [8]. The code solves (2.1)–(2.4) using finite elements with quadratic basis functions. In order to resolve the boundary layer, the domain was discretized into sixty fixed but unequally spaced elements, with more elements placed near $x = 0$.

Application of the finite element method to the model results in a system of nonlinear coupled ODEs for the nodal values of concentration and stress. The system of ODEs was integrated in time using a stiff DAE solver, DASSL [42]. DASSL uses an Adams–Bashforth–Moulton predictor-corrector algorithm with a variable-order backward differentiation formula. The corrector is implicit and the nonlinear system is solved by Newton's method with an analytical Jacobian matrix. The time step is automatically updated to control the estimated error within a specified tolerance. The error tolerance and number and distribution of elements were adjusted until the results were insensitive to the size of these parameters.

5.1. Comparison with asymptotics. The parameters chosen for use in both the analytical model and the numerical simulations were as follows:

$$C_* = 1/2, \qquad D_{\mathrm{r}} = 4, \qquad C_{\mathrm{ext}} = 1/4, \qquad L = 3, \qquad D_{\mathrm{g}} = 4 \times 10^{-4}, \tag{5.1a}$$

$$\beta_{\mathrm{g}} = 1, \qquad \beta_{\mathrm{r}} = 10^4, \qquad \alpha = 80, \qquad k = 1.33 \times 10^4. \tag{5.1b}$$

These parameters essentially correspond to an ϵ value of 10^{-4}. Also, with these parameters, $s_0 \approx 0.4550$.

Figure 5.1 shows a comparison of the asymptotic and numerical predictions of the front position for small time. The speed of the front decreases with time as predicted by both methods. The agreement between the asymptotic and numerical results is excellent.

In Figure 5.2 we show a graph of the concentration for the parameters in (5.1) and the times listed. The interval in x is restricted near $x = 0$; the grid spacing decreases as we reach that endpoint. There is excellent agreement between the numerical and outer solutions in the region away from the boundary layer, and the discontinuity in

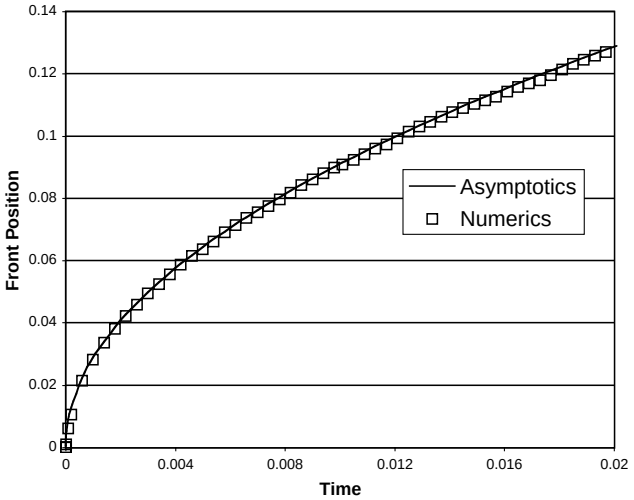

FIG. 5.1. *Asymptotic and numerical calculations of $s(t)$ for the parameters in* (5.1).

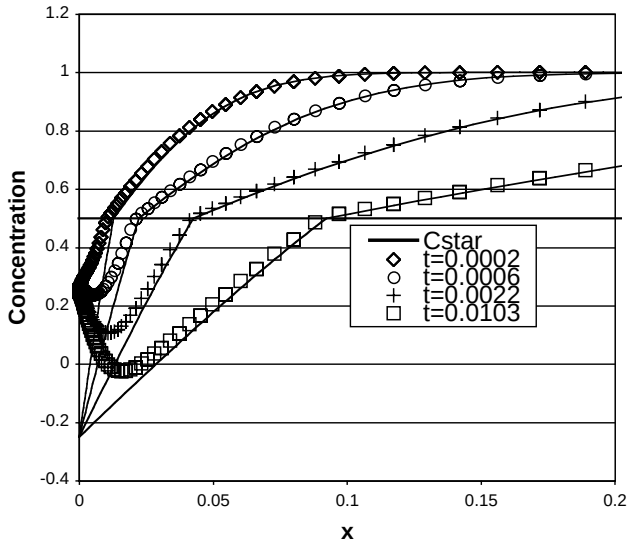

FIG. 5.2. *Aymptotic solution $C_0(x,t)$ (lines) and numerical solution (symbols) versus x. The numerical and asymptotic solutions are indistinguishable beyond $x = 0.2$.*

$\partial C/\partial x$ at the glass-rubber transition is accurately predicted by both techniques. Note that at $t = 0.0103$ even the numerical solution goes negative, so we have confirmed that negative concentration values are not an artifact of the asymptotic solution. We shall examine the root causes of this phenomenon in the next section.

Figure 5.3 shows a graph of the stress versus x for the times listed. There is excellent agreement between the asymptotic and numerical solutions for the glassy stress. In addition, the zero-stress approximation (3.8) and the numerical calculation

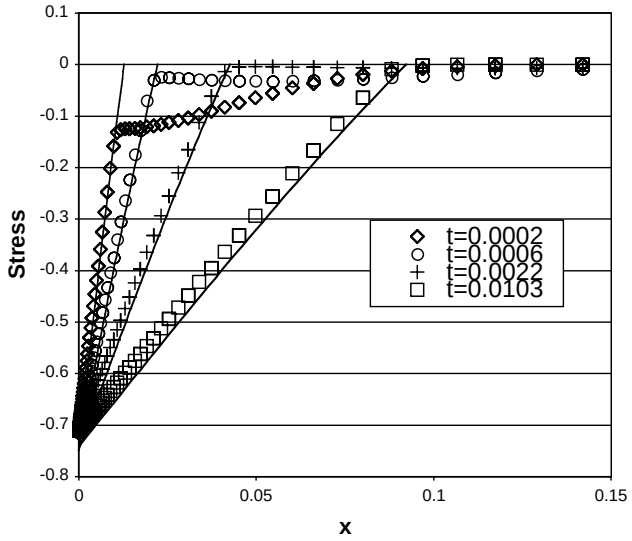

FIG. 5.3. *Aymptotic solution $\sigma_0^{\mathrm{g}}(x,t)$ (lines) and numerical solution (symbols) versus x. The rubbery stress is zero. The numerical and asymptotic solutions are indistinguishable beyond $x = 0.15$.*

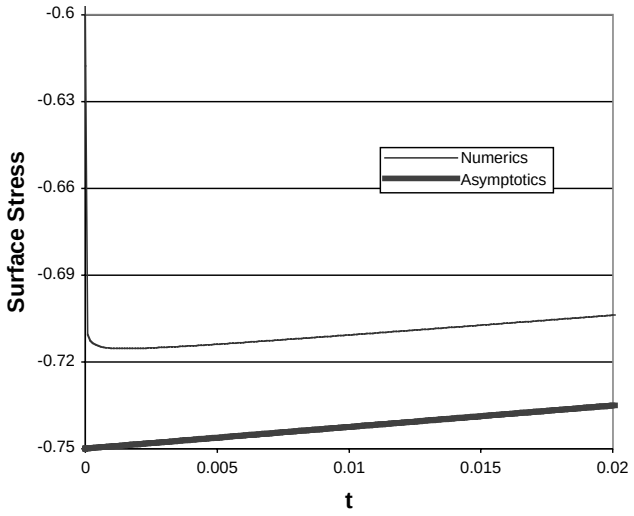

FIG. 5.4. *Comparison of asymptotic (from equation* (3.6)*) and numerical expressions for surface stress.*

in the rubbery region match for larger times. From the graph at $t = 2 \times 10^{-4}$ we see that due to the rapid drop in C at the surface, the stress in the rubbery region is initially $O(1)$, as shown in section 4.2. For longer times, the stress decays exponentially as predicted by (4.11b), until at $t = 2.2 \times 10^{-3}$, the numerical calculation is virtually indistinguishable from (3.8).

Figure 5.4 shows a graph of the surface stress at $x = 0$. Though the outer and numerical solutions decay on the same e^{-t} scale, there is a persistent gap because the outer solution in (3.6) assumes an instantaneous change in C at $t = 0$, while the numerical simulations follow (2.4b). Thus, initially the surface concentration and surface stress evolve on a time scale roughly proportional to k^{-1}. This time scale will become important later on when we examine the reason for the negative concentration values.

5.2. Long-time results. Though the validity of the asymptotics ends for moderate times, we can certainly continue the numerical calculations into that region. Figure 5.5 shows the computed concentration profiles for various times. Note that between $t = 2$ and $t = 4$, the film becomes entirely glassy. (For more discussion of the time at which the front reaches the back of the film, see the appendix.) Since the glass has a longer relaxation time, the change in the concentration between $t = 2$ and $t = 4$ is relatively small.

The unphysical negative concentration is not a brief anomaly; it continues for moderate time, and the size of the dip actually increases. It should be noted that the desorption overshoot disappears if k is smaller, which corresponds to a slower change in the surface concentration. For more discussion of this topic, see section 6.

Figure 5.6 shows the computed stress profiles for the same series of times. The nearly linear stress in the glassy region implies a constant non-Fickian flux. Thus, the evolution of the concentration in this region is dominated by the Fickian flux. Note that the surface stress continues its exponential decay to a final limiting value of zero.

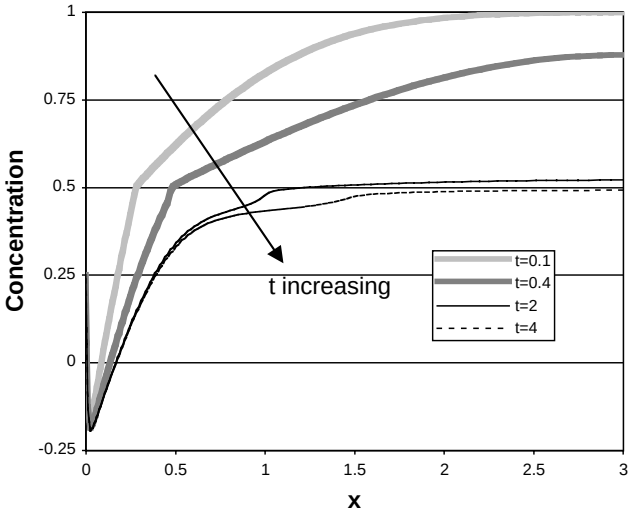

FIG. 5.5. *Computed concentration profiles versus x for the times listed in the legend.*

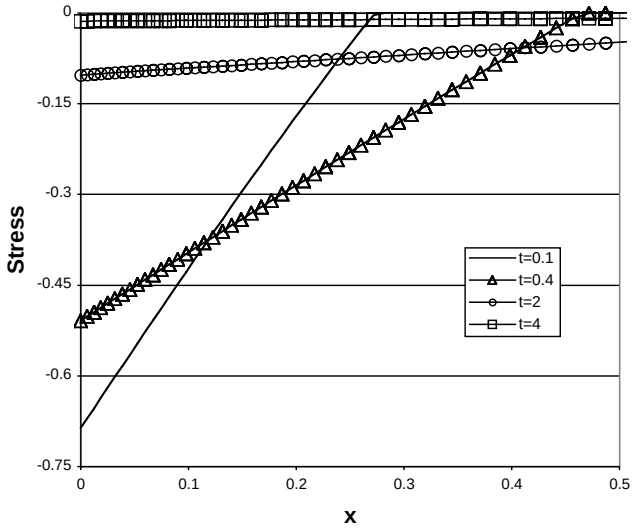

FIG. 5.6. *Computed stress profiles versus x for the times listed in the legend.*

6. Explaining negative concentrations. The unphysical negative concentration is not an artifact of the asymptotics, as the numerical solutions in Figure 5.2 show. To explain the phenomenon, we solve (2.6b) for short times, using (3.6) and (3.2). After some work, we obtain the following expression:

$$\lim_{x\to 0} C_0^{\mathrm{g}}(x,t) = \lim_{t\to 0} \sigma^{\mathrm{g}}(0,t) + C_*. \tag{6.1}$$

Hence the discontinuity *in the outer solution* exists for all time unless

$$\lim_{t\to 0} \sigma^{\mathrm{g}}(0,t) = C_{\mathrm{ext}} - C_*. \tag{6.2}$$

Moreover, the concentration will go negative whenever

$$\lim_{t\to 0} \sigma^{\mathrm{g}}(0,t) < -C_*. \tag{6.3}$$

How then to avoid satisfying this condition?

Following common practice for diffusion and heat transfer problems, we took $k \to \infty$ in (2.4b) to obtain the Dirichlet condition (3.4). The resulting discontinuous jump at $t = 0$ forces $\sigma(0, 0^+) = C_{\mathrm{ext}} - 1$, as can be seen from (3.6), and this value can violate (6.3). Why does the standard Dirichlet trick not work for this model?

In a standard diffusion problem, lines of constant t are characteristics. Thus these equations transmit disturbances with infinite signal speed to the entire domain. As can be intuited from the leading-order outer equations (3.3) and (3.9a), the same is true for this model. This explains why the solution does not break down in any mathematical sense; it just goes negative, which offends our physical sensibilities.

The key difference rather is the delay term inherent in (2.1b). When a jump occurs very quickly, the stress cannot relax fast enough (even with an $O(\epsilon)$ relaxation time in the rubber) to equilibrate it. Once a large stress gradient has been introduced at the exposed surface, there is no mechanism in (3.2a) to stop the concentration from going negative. This is related to the observation in [41] that other models for anomalous diffusion will have negative concentration values if a "retardation time" is not included.

There are several mechanisms one can introduce to moderate the concentration dip. For instance, consider the case where the $\partial\sigma/\partial x$ term in (2.1a) is multiplied by a "stress diffusion coefficient" $E(C)$, where $E(0) = 0$. This term would remain at leading order in the equation analogous to (3.2a), causing $\partial C_0^{\mathrm{g}}/\partial t(C = 0) = 0$ and preventing the concentration from going negative. Moreover, preliminary numerical calculations indicate that if $E(C) \ll 1$ in the glassy region, this change can eliminate negative concentrations while maintaining desorption overshoot.

Another remedy is to slow the change so that it occurs on the fast relaxation time scale of the rubbery polymer. Thus we replace (3.4) by

$$C(0,\tau) = C_{\mathrm{ext}} + (1 - C_{\mathrm{ext}})e^{-\lambda\tau}, \qquad \lambda \neq 1, \tag{6.4}$$

where τ is the time scale defined in (4.10). The exponential form is chosen to match the analysis in Edwards [24] and the forms in Hui et al. [34] and Long and Richman [43]; $\lambda \neq 1$ is taken for simplicity. As λ increases, the driving force increases and the transition between rubber and glass steepens.

As given by (6.4), the interface is now rubbery for some interval. We may substitute (6.4) into the leading orders of (2.6b) and (2.7b) and solve to obtain the stress boundary condition. Since τ is an initial-layer variable, we may take the limit of this condition as $\tau \to \infty$ to find the limiting value of the outer boundary condition. This is found to be

$$\lim_{t\to 0} \sigma^{\mathrm{g}}(0,t) = -\frac{C_* - C_{\mathrm{ext}}}{1-\lambda} + \frac{\lambda(1 - C_{\mathrm{ext}})}{1-\lambda}\left(\frac{C_* - C_{\mathrm{ext}}}{1 - C_{\mathrm{ext}}}\right)^{1/\lambda}. \tag{6.5}$$

Thus our matching condition, and hence $C^{\mathrm{g}}(x, 0)$, depends on λ. As $\lambda \to \infty$, (6.4) approaches a step function and our result from section 3 holds:

$$\lim_{t\to 0} \sigma^{\mathrm{g}}(0,t) = -(1 - C_{\mathrm{ext}}), \qquad \lambda \to \infty. \tag{6.6a}$$

If instead $\lambda \to 0$, we obtain the following:

$$\lim_{t\to 0} \sigma^{\mathrm{g}}(0,t) = -(C_* - C_{\mathrm{ext}}), \quad \lambda \to 0, \tag{6.6b}$$

which from (6.2) is exactly the condition required to eliminate the boundary layer at the exposed surface. In this case the exterior concentration varies on a time scale slower than that of the rubber relaxation time, so the *entire* polymer can equilibrate to the exterior.

Last, we note that from (6.3) that in order to maintain a positive concentration, the expression in (6.5) must be greater than $-C_*$. Hence the generation of negative concentrations in our model can be remedied by imposing more physically realistic boundary conditions. If changes in the exterior happen on a faster time scale than the rubber relaxation time scale, the surface cannot immediately equilibrate. Thus, the polymer exhibits a sort of "self-regulation" which puts restrictions on the speed at which the surface concentration can change. This sort of self-regulation has been seen in similar models of sorption processes [24].

7. Conclusions. During the desorption of saturated polymers near the glass-rubber transition temperature, a glassy skin will form near the exposed surface. One mechanism for the formation of such a skin is viscoelastic relaxation in the polymer network. The mathematical model presented here has captured this behavior in previous numerical [5], [8] and analytical [26], [29] studies. However, never before has the model been studied in both ways simultaneously. This merging of techniques involved restricting the analytical study to a more realistic finite domain and adapting the numerical parameter scheme to approximate a piecewise-constant approach. By approaching the solution in two ways, we validated both approaches. In particular, we established that negative concentrations were the result of neither a computational bug nor an erroneous asymptotic approximation, but were rather the predictable and robust result of a mathematically simple, but physically unrealistic, boundary condition.

In the asymptotic work, the parameters are taken as piecewise constant and the system is treated in a manner similar to a Stefan problem. Since the system is not amenable to similarity solutions, an integral method based on the one in Boley [38] is used. The finite domain is extended to a semi-infinite one in both cases, and the method of images is used to handle the insulated boundary condition at $x = L$.

The asymptotic and numerical results match well, showing a quick transition to the glassy region near the exposed surface. The glass-rubber interface initially moves like $t^{1/2}$, reflecting the fact that the viscoelastic memory effects have not yet had time to develop. The numerical solutions demonstrated desorption overshoot, where a minimum in the concentration occurs in the interior of the domain. This is mirrored in the asymptotic outer solution, which is less than the imposed surface concentration as $x \to 0$.

The overshoot can be traced to our replacement of a flux balance condition with a Dirichlet condition. Such approximations are routinely used in diffusion and heat conduction problems instead of the more complicated (but physically realistic) activity or flux conditions. However, in our case taking the limit of large k leads to negative concentrations. Essentially, we are attempting to force the surface concentration to vary faster than the polymer can adapt. The intrinsic time scale in the model then reduces the set of boundary conditions that can lead to physically meaningful results.

In section 6 we proposed two remedies for negative concentrations. A stress diffusion coefficient can be introduced which shuts down further penetrant diffusion

when the polymer is dry. Alternatively, if we vary the surface concentration on the fast τ time scale, we eliminate the negative concentrations. Essentially, the τ-variance is the fastest that the actual physical system can accommodate. This type of self-regulation has been demonstrated in sorption models [24].

Though the numerical and asymptotic profiles match well for small t, the appendix shows that due to the diffusive nature of the operators considered, the fictitious boundary conditions must be approximated very closely to guarantee accurate results for moderate t. Nevertheless, the agreement for small time provides a sturdy background on which to base further work. Not only do the asymptotic solutions verify the numerics, but they also demonstrate parameter ranges which produce unphysical results.

Appendix. Some remarks on the intersection point. We conclude by examining the solution near the time $t = t_L$ where $s(t_L) = L$. Due to the symmetry about the line $x = L$, $s^{-1}(x)$ should be even about $x = L$, so the first terms in our expansion for $s(t)$ should be

$$s(t) \sim L - s_1\sqrt{r}, \qquad r = t_L - t > 0, \qquad s_1 > 0. \tag{A.1}$$

Using (3.10a) and (A.1) in (3.11), we may construct an expansion in r, eventually reaching the following terms at $O(r)$:

$$(s_1^2 - 2D_{\mathrm{r}})\frac{\partial^2 T^{\mathrm{r}}}{\partial x^2}(L, t_L) = 0, \tag{A.2a}$$

$$\left(\frac{s_1^2}{2} - 1\right)\frac{\partial^2 \sigma_0^{\mathrm{g}}}{\partial x}(L, t_L) = 0. \tag{A.2b}$$

It can be shown that if the second derivative of T^{r} vanishes at $x = L$, *all* even derivatives of T^{r} must vanish there. But the numerical solutions shown later in Figure A.1 do not support this transcendental vanishing. Thus, we set $s_1 = \sqrt{2D_{\mathrm{r}}}$.

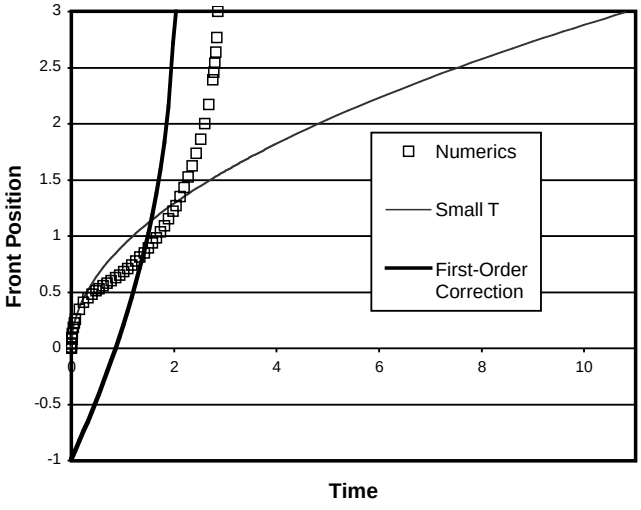

FIG. A.1. *Comparison of short- and intersection-time expressions for $s(t)$ with true front position. Here $s_1 = \sqrt{8}$, $s_L = 1.0634$, and $t_L = 1.990$.*

(Formally, this must be done in a limiting way by setting the stress in the glass equal to a small quantity representing σ_1^{r}, then taking that term to zero.)

To determine t_L, we introduce another degree of freedom into our fictitious condition as follows:

$$f^{\mathrm{i}}(x) \sim f_0^{\mathrm{i}} + f_1^{\mathrm{i}} x. \tag{A.3}$$

Substituting (A.3) into (3.10a) using (4.8), we may combine the resulting equations to obtain the following equation involving t_L:

$$\operatorname{erf} s_0 = \operatorname{erf} s_L - \frac{2s_L}{\sqrt{\pi}} e^{-s_L^2}, \qquad s_L = \frac{L}{2\sqrt{t_L}}. \tag{A.4}$$

Note the underlying parabolic nature of the operator, as evidenced by the relationship between the definition of s_L and the diffusion equation similarity variable. It can be shown that (A.4) has exactly one root s_L. In addition, $s_L > s_0$, so the front must speed up as time passes. Figure A.1 shows a graph of the short- and intersection-time expressions for $s(t)$ as compared with the numerical calculations.

By replacing the one-term expansion for $f^{\mathrm{i}}(x)$ with a two-term expression, we obtain closer agreement near $x = L$, as desired. In particular, we note that by combining the asymptotic results, we obtain the change in concavity of the graph and an acceptable estimate of the inflection time.

Unfortunately, though the two-term expansion provides an improved estimate of t_L, it is still not very accurate. Due to the diffusive nature of the underlying problem, the estimate of the initial condition must be highly accurate to obtain reasonable predictions for moderate t. In addition, the constructed solution does not work well for small times ($r = O(1)$). Thus, as a next step one should construct a three-term expansion for $f^{\mathrm{i}}(x)$ that satisfies the leading-order conditions at both $x = 0$ and $x = L$. This sort of iterative process, where one continually improves the form of f^{i}, should converge to the correct solution on finite domains. Infinite domains are fundamentally different since $t \to \infty$. This case can be treated asymptotically using appropriately chosen expansion functions [26], [29], [39], [40].

Acknowledgments. We thank the reviewers for many helpful comments that improved the manuscript.

REFERENCES

[1] N. Thomas and A. H. Windle, *Transport of methanol in poly-(methyl-methocry-late)*, Polymer, 19 (1978), pp. 255–265.

[2] M. Vinjamur and R. A. Cairncross, *A high airflow drying experimental set-up to study drying behavior of polymer solvent systems*, Drying Tech. J., 19 (2001), pp. 1591–1612.

[3] M. Vinjamur and R. A. Cairncross, *Experimental investigations of trapping skinning*, J. Appl. Polym. Sci., 83 (2002), pp. 2269–2273.

[4] M. Vinjamur and R. A. Cairncross, *A non-Fickian non-isothermal model to predict anomalous trapping skinning behaviour during drying of polymer coatings*, AIChE J., to appear.

[5] M. Vinjamur and R. A. Cairncross, *Guidelines for dryer design based on results from non-Fickian model*, J. Appl. Polym. Sci., to appear.

[6] R. A. Cairncross, L. F. Francis, and L. E. Scriven, *Competing drying and reaction mechanisms in the formation of sol-to-gel films, fibers, and spheres*, Drying Tech. J., 10 (1992), pp. 893–923.

[7] R. A. Cairncross, L. F. Francis, and L. E. Scriven, *Predicting drying in coatings that react and gel: Drying regime maps*, AIChE J., 42 (1996), pp. 55–67.

[8] R. A. Cairncross and C. J. Durning, *A model for drying of viscoelastic coatings*, AIChE J., 42 (1996), pp. 2415–2425.

[9] E. Ben-Yoseph and R. W. Hertel, *Computer modeling of sugar crystallization during drying of thin sugar films*, J. Crys. Growth, 198/199 (1999), pp. 1294–1298.
[10] E. Ben-Yoseph, R. W. Hertel, and D. Howling, *Three dimensional model of phase transition of thin sucrose films during drying*, J. Food Eng., 44 (2000), pp. 13–22.
[11] S. Simal, A. Femenia, P. Llull, and C. Rossello, *Dehydration of aloe vera: Simulation of drying curves and evaluation of functional properties*, J. Food Eng., 43 (2000), pp. 109–114.
[12] J. Crank, *The influence of concentration-dependent diffusion on rate of evaporation*, Proc. Phys. Soc., 63 (1950), pp. 484–491.
[13] J. Crank, *Diffusion in media with variable properties, part* III: *Diffusion coefficients which vary discontinuously with concentration*, Trans. Faraday Soc., 47 (1951), pp. 450–461.
[14] C. A. Finch, ed., *Chemistry and Technology of Water-Soluble Polymers*, Plenum Press, New York, 1983.
[15] W. R. Vieth, *Diffusion in and Through Polymers: Principles and Applications*, Oxford University Press, Oxford, 1991.
[16] J. S. Vrentas, C. M. Jorzelski, and J. L. Duda, *A Deborah number for diffusion in polymer-solvent systems*, AIChE J., 21 (1975), pp. 894–901.
[17] M. Dabral, *Solidification of Coatings: Theory and Modeling of Drying, Curing, and Microstructure Growth*. Ph.D. thesis, University of Minnesota, Minneapolis-St. Paul, MN, 1999.
[18] N. O. Ngu and S. K. Mallapragada, *Quantitative analysis of crystallization and skin formation during isothermal solvent removal from semicrystalline polymers*, Polymer, 40 (1999), pp. 5393–5400.
[19] I. H. Romdhane, P. E. Price, Jr., C. A. Miller, P. T. Benson, and S. Wang, *Drying of glassy polymer films*, Ind. Eng. Chem. Res., 40 (2001), pp. 3065–3075.
[20] H. L. Frisch, *Sorption and transport in glassy polymers—a review*, Polymer Engr. Sci., 20 (1980), pp. 2–13.
[21] D. R. Paul and W. J. Koros, *Effect of partially immobilizing sorption on permeability and diffusion time lag*, J. Polym. Sci., 14 (1976), pp. 675–685.
[22] W. R. Vieth and K. J. Sladek, *A model for diffusion in a glassy polymer*, J. Colloid Sci., 20 (1965), pp. 1014–1033.
[23] J. Crank, *The Mathematics of Diffusion*, 2nd ed., Clarendon Press, Oxford, 1976.
[24] D. A. Edwards and D. S. Cohen, *A mathematical model of a dissolving polymer*, AIChE. J., 41 (1995), pp. 2345–2355.
[25] D. A. Edwards and D. S. Cohen, *An unusual moving boundary condition arising in anomalous diffusion problems*, SIAM J. Appl. Math., 55 (1995), pp. 662–676.
[26] D. A. Edwards, *Skinning during desorption of polymers: An asymptotic analysis*, SIAM J. Appl. Math., 59 (1999), pp. 1134–1155.
[27] C. J. Durning, *Differential sorption in viscoelastic fluids*, J. Polym. Sci. B, 23 (1985), pp. 1831–1855.
[28] C. J. Durning and M. Tabor, *Mutual diffusion in concentrated polymer solutions under a small driving force*, Macromolecules, 19 (1986), pp. 2220–2232.
[29] D. A. Edwards, *A mathematical model for trapping skinning in polymers*, Stud. Appl. Math. (1997), pp. 49–80.
[30] J. C. Wu and N. A. Peppas, *Modeling of penetrant diffusion in glassy polymers with an integral sorption Deborah number*, J. Polym. Sci. B, 31 (1993), pp. 1503–1518.
[31] T. P. Witelski, *Traveling wave solutions for case* II *diffusion in polymers*, J. Polym. Sci. B, 34 (1996), pp. 141–150.
[32] H. L. Frisch, T. K. Kwei, and T. T. Wang, *Diffusion in glassy polymers*, II, J. Polym. Sci. A-2, 7 (1969), pp. 879–887.
[33] S. Mehdizadeh and C. J. Durning, *Predictions of differential sorption kinetics near T_g for benzene in polystyrene*, AICHE J., 36 (1990), pp. 877–884.
[34] C. Y. Hui, K. C. Wu, R. C. Lasky, and E. J. Kramer, *Case* II *diffusion in polymers.* I. *Transient swelling*, J. Appl. Phys., 61 (1987), pp. 5129–5136.
[35] C. Y. Hui, K. C. Wu, R. C. Lasky, and E. J. Kramer, *Case* II *diffusion in polymers.* II. *Steady state front motion*, J. Appl. Phys., 61 (1987), pp. 5137–5149.
[36] N. Thomas and A. H. Windle, *A deformation model for case* II *diffusion*, Polymer, 21 (1980), pp. 613–619.
[37] D. S. Cohen and A. B. White, Jr., *Sharp fronts due to diffusion and stress at the glass transition in polymers*, J. Polymer Sci. B, 27 (1989), pp. 1731–1747.
[38] B. A. Boley, *A method of heat conduction analysis of melting and solidification problems*, J. Math. Phys., 40 (1961), pp. 300–313.
[39] D. A. Edwards, *Constant front speed in weakly diffusive non-Fickian systems*, SIAM J. Appl. Math., 55 (1995), pp. 1039–1058.

[40] D. A. Edwards, *The effect of a varying diffusion coefficient in polymer-penetrant systems*, IMA J. Appl. Math., 55 (1995), pp. 49–66.

[41] N. S. Kalospiros, R. Ocone, G. Astarita, and J. H. Meldon, *Analysis of anomalous diffusion and relaxation in solid polymers*, Ind. Eng. Chem. Res., 30 (1991), pp. 851–864.

[42] L. R. Petzold, *A Description of DASSL: A Differential/Algebraic System Solver*, Sandia technical report 82-8637, Sandia National Laboratories, Livermore, CA, 1982.

[43] F. A. Long and D. Richman, *Concentration gradients for diffusion of vapors in glassy polymers and their relation to time dependent diffusion phenomena*, J. Am. Chem. Soc., 82 (1960), pp. 513–519.